

Effect of El-Niño Southern Oscillation (ENSO) on Heat Transport in The Indonesia Throughflow Passages and Ocean Heat Content in The Banda Sea

Khafid Rizki Pratama^{1,5*}, Ivonne Milichristi Radjawane^{1,2,3}, Bayu Edo Pratama^{4,5}

¹Earth Science Study Program, Faculty of Earth Science and Technology, Bandung Institute of Technology

²Oceanography Research Group, Faculty of Earth Science and Technology, Bandung Institute of Technology
Labtex XI, ITB Campus, Jl. Ganesa, Bandung-Jawa Barat, Indonesia

³Korea-Indonesia Marine Technology Cooperation Research Center
Jl. Fatahillah No. 24 Cirebon-Jawa Barat 45611, Indonesia

⁴Université de Bretagne Occidentale
3 rue des Archives, CS 93837, Brest, Finistere F29238, France

⁵Indonesia Agency for Meteorology Climatology and Geophysics
Jl. Angkasa 1 No.2, RT.1/RW.10, Kec. Kemayoran, Jakarta 10610 Indonesia
Email: khafidrizkipratama@gmail.com

Abstract

Indonesia Throughflow (ITF) flows water mass from the Northern Pacific Ocean to the Indian Ocean through Indonesian waters. This research was conducted in the Eastern Indonesia waters in 2009–2019 using Copernicus Marine Environment Monitoring Service (CMEMS) reanalysis and World Ocean Database (WOD) to analyze heat transport in ITF passages and ocean heat content in the Banda Sea. The analysis shows that ITF and heat transport have a strong relationship with a correlation of 0.7 during El-Niño Southern Oscillation (ENSO). Regarding the vertical profile by depth, heat transport in the Makassar Strait during La Niña was detected to be stronger in the Labani Channel and Central Sulawesi water, with values of -1.2 PW and -0.6 PW. Then, in the Lifamatola Strait, it was identified as strengthening in the Lifamatola Channel and Halmahera Strait with a value of -0.5 PW and -0.3 PW. The lag correlation between heat transport and the Oceanic Niño Index (ONI) shows a lag time of around 3-4 months, with the ENSO preceding heat transport. Mixed layer depth has an inverse relationship and salinity has a direct relationship with ENSO. Meanwhile, salinity has a relationship that is directly proportional to the ENSO. Another influence is the Rossby (Kelvin) waves when La Niña (El Niño) propagates to the West (Central) Pacific region, which tends to cause higher (lower) sea level elevations so that ITF and heat transport become strong (weak). It causes the ocean heat content (OHC) to increase during La Niña and decrease during El Niño.

Keywords: ITF, heat transport, ocean heat content, ENSO

Introduction

One of the most famous circulations on the Maritime Continent is the Indonesian Throughflow (ITF). ITF flows water mass from the Pacific Ocean to the Indian Ocean through Indonesian waters (Gordon and McClean, 1999; Gordon and Susanto, 2001). This circulation continuously pumps water masses into Indonesian waters caused by gradient differences (Sprintall and Revelard, 2014). The flow of water mass causes several ocean patterns in Indonesia to change in terms of ocean dynamics and their impact on climate (Gordon et al., 2010). The ITF is divided into three entry points, namely, the western passage through the Karimata Strait, the middle passage through the Makassar Strait, and the eastern passage through the Lifamatola Strait. The middle and eastern passages carry the maximum Sverdrup transport, ranging from -4 to -12 Sv (1 Sv = $1 \times 10^6 \text{ m}^3\text{s}^{-1}$). Both flow into the Banda Sea before heading to the Indian Ocean, and some exit through

the Lombok, Bali, and Flores Straits (Sprintall et al., 2014). ITF transport variations are known to have complex variability. ENSO influences the ITF variability on an interannual scale. On the other hand, the monsoon that blows across the Maritime Continent affects ITF transport and its barotropic circulation (Meyers, 1996). The northwest (Indo-Asian) and southeast (Indo-Australian) monsoons have a direct impact on transport through the Makassar Strait due to the influence of the atmosphere on sea surface height (Napitu et al., 2018). In addition, Field and Gordon (1992) found that the water mass from the Pacific Ocean has a residence time that varies in the Banda Sea.

The residence time is caused by mixing that occurs throughout the year and the influence of factors such as tidal mixing, turbulence, and changes in the monsoon winds (Gordon, 2012; Pujiana et al., 2012). A study conducted by Gordon and McClean (1999) also found that the Banda Sea was influenced

by southeast and northwest monsoons, which resulted in changes in thermohaline stratification. During the northwest monsoon (southeast monsoon), the water mass from the Flores Sea predominates at a depth of 150 (100) meters, while the water mass from the Halmahera Strait occurs at a depth of 100 (150) meters, and the reverse situation occurs when the east monsoon is active (Haryanto *et al.*, 2021; Purwanto *et al.*, 2021). The mean transport in the straits that empties into the Banda Sea has a value of -3 Sv to +1.5 Sv, and the identification in the Timor Strait has a transport value of -7,5 Sv to -3 Sv. It is dominated by intraseasonal time scales (Masoleh and Atmadipoera, 2018). The Banda Sea has diverse characteristics in terms of topography and oceanographic conditions (Wijaya *et al.*, 2018). Several events, such as tropical cyclones, have occurred in the Banda Sea with confirmed impacts from an infrastructure and social perspective (Nugroho and Muzaki, 2021).

This study focuses on analyzing the contributions of ITF, heat transport, and ocean heat content to ocean conditions in the Banda Sea. The components of the analysis carried out involved locations in the Makassar Strait and the Lifamatola Strait.

Materials and Methods

This research is located at the coordinates 1° 0' 0" S to 11° 0' 0" S and 122° 0' 0" E to 133° 0' 0" E, as shown in Figure 1. The selection of these

coordinates is based on the dominance of the influence of El Niño Southern Oscillation (ENSO) variability, in which the Banda Sea and its surroundings are the main waters in the eastern part of Indonesia and contribute to changes in the weather and climate (Pei *et al.*, 2021). The "red box" is the Banda Sea, which is examined for parameters affected by heat transport. Points A and B are the coordinates of the Makassar Strait and the Lifamatola Strait, which are locations for analysis of ITF and heat transport with an average depth of 0 to 300 meters below sea level.

The reanalysis data used in this study from the Copernicus Global Ocean Physics Reanalysis (GLORYS12V) with a spatial resolution of 1/12° (8 km x 8 km). The data selection is based on the dataset's characteristics, which have assimilated input from in-situ observation data (Roman-Stork *et al.*, 2020). In addition, observation data from the World Ocean Database (WOD) is used as validation with model reanalysis. Prior validation was performed in this study to compare the reanalysis obtained from the Copernicus Global Ocean Product Reanalysis and in-situ observation data from the National Center for Environmental Information/World Ocean Database (NCEI/WOD).

Validation was carried out using sub-surface temperature, and salinity plotted into the vertical profile, as well as statistical methods that included the correlation coefficient (Corr), root mean square error (RMSE), and bias whose mathematical formulas are shown in Equations 1–3 (Wang *et al.*, 2022).

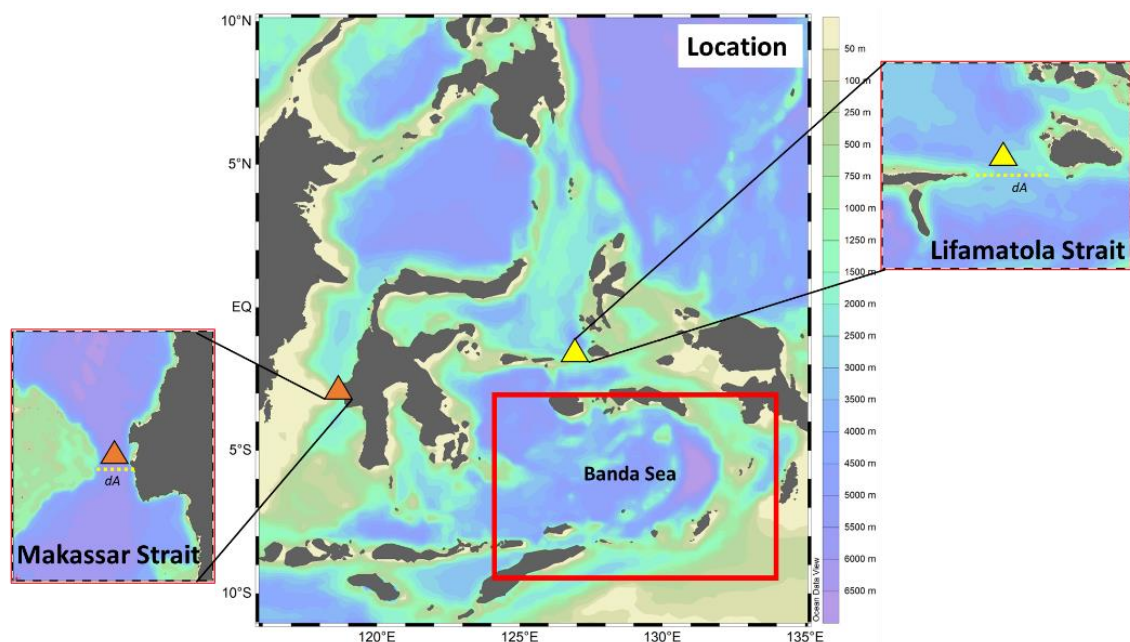


Figure 1. Research location in Eastern Indonesia water. Red box is Banda Sea

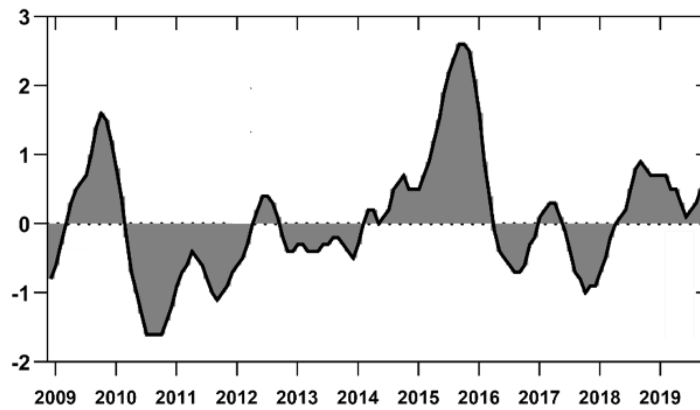


Figure 2. Oceanic Niño Index (ONI) in 2009-2019

$$= \frac{\sum_{i=1}^n (x_i - \bar{x})(y_i - \bar{y})}{\sqrt{\sum_{i=1}^n (x_i - \bar{x})^2 \sum_{i=1}^n (y_i - \bar{y})^2}} \quad (1)$$

$$RMSE = \sqrt{\frac{\sum_{i=1}^n (x - y)^2}{n}} \quad (2)$$

$$bias = (\bar{y} - \bar{x}) \quad (3)$$

where n is the amount of data, i is the data sequence, x and y are the model and observation data, and \bar{x} and \bar{y} are the averages of the model and observation data, respectively. The calculation of ITF transport using the previous formulation has been used by Nanlohy *et al.* (2018) as follows:

$$Sv = V \times dA \quad (4)$$

where V is the value of the meridional current velocity ($m \cdot s^{-1}$), and dA is the cross-sectional of the study area (m^2). Transport values are calculated monthly averages and filtered using the low-pass filter method (cut-off 13 months). Filter data determines the relationship between ENSO variability and ITF transport. To analyze heat transfer in the two straits, use the formulation that has been done by Katavouta *et al.* (2022), as follows:

$$HT = Cp \int \rho_{(p,s,t)} \theta v dA \quad (5)$$

where ρ is the density of water, Cp is the specific heat capacity of water at constant pressure, h_1 is the top depth (0 meters), h_2 is the bottom depth (300 m), and θ is the potential temperature in $^{\circ}C$.

The evidence of changes in monthly frequency during ITF propagation and heat transport in the two straits that emptied into the Banda Sea was compared. Power spectral density (PSD) is used for salinity and mixed layer depth (MLD) as a method to

determine the period of recurrence variability. Empirical Orthogonal Function (EOF) method by applying principal component (PC) values that have been normalized. The resulting value will be temporally anomalous. Analysis to determine the lag time that occurs between the anomaly and the ONI index (Figure 2) uses the following formulation:

$$r = \frac{\sum_{i=1}^n (x_i - \bar{x}) - (y_i - \bar{y})}{\sqrt{\sum_{i=1}^n (x_i - \bar{x})^2 - (y_i - \bar{y})^2}} \quad (6)$$

where n is the amount of data, x and y are the variables x and y in 1, and \bar{x} and \bar{y} are the average values of the variables x and y . The results of the formulation will produce relationships and time-lag correlations.

Result and Discussion

Reanalysis data from CMEMS was compared with observation data from the World Ocean Database (WOD). As for the observation data instrument, it uses data taken from the profiling float, which is also abbreviated as PFL.

Figure 3a and 3b shows a data plot comparing sub-surface temperature and salinity in the Makassar Strait on September 23, 2013. The data comparison results show a correlation value of 0.9673, a RMSE 0.16 $^{\circ}C$, and a bias 0.19 $^{\circ}C$. Comparing the sub-surface salinity shows a correlation value of 0.77, an RMSE 0.63 PSU, and 0.62 PSU. The results of the two datasets show the similarity of the corr, RMSE, and bias values, which means that the CMEMS reanalysis data is categorized as good (Sotillo *et al.*, 2021).

The heat transport is related to the calculation results of ITF's transport over 10 years. Improvements in the calculation of heat transport combine research

that has been carried out by Vranes *et al.* (2002) and Katavouta *et al.* (2022). The calculations taken from these studies are the cross-sectional area of each point passed by ITF to determine the process of heat flowing from the Pacific Ocean, considering the specific heat. A comparison between heat transport and ITF transport in the Makassar Strait shows that there are fluctuations, and they tend to follow almost the same pattern. In 2011, the ONI index recorded a weak La Niña. The same thing is shown by the graphs in Figures 4a and 4b, which the heat transport has a large negative transport value, indicating a strong flow. Whereas in 2015, which was seen as a strong El Niño event, there was a tendency for a small negative value to indicate weaker flows. In 2017, the value of heat transport tends to be strong, and together with La Niña events, the weak category is based on the ONI index. The comparison of these graphs confirms the research conducted by Vranes *et al.* (2002). The relationship between heat transport and ITF transport in the Makassar Strait is believed to affect sub-surface temperatures in the Banda Sea, where research conducted by Gordon *et al.* (2005) found that sea surface temperature (SST) in the Banda Sea is related to the mass of water from ITF that empties into the Banda Sea.

Another condition seen in the Lifamatola Strait is ENSO variability, which has a significant influence on fluctuations in heat transport to the Banda Sea. The identified heat transport is almost in balance with ENSO events. This relationship can be seen from the La Niña events in 2011-2012, where heat transport increased along with the ITF strengthening. This pattern follows research conducted by Sprintall *et al.* (2009), who found that the heat transport that flows

from the Pacific Ocean to the Indian Ocean tends to transport heat and change salinity so that it changes the water mass in the Banda Sea. The reverse condition occurred in 2015–2016, an El Niño event. Heat transport tends to weaken with a value of -0.3 to -0.2 PW (negative is stronger to Banda Sea), and ITF has a value of +0 to +1 Sv (positive is weaker to Banda Sea). In that year, it was identified that there was no active cyclone in the Banda Sea. This is probably caused by the ocean's heat decreasing and becoming unable to develop into convective clouds (Roman Stork *et al.*, 2020). Whereas in 2017–2018, there was a weak La Niña. The pattern of heat transport was identified that flowed stronger with a value of -0.7 to -0.8 PW and ITF transport ranging from -0.6 to -0.7 Sv. This demonstrates the relationship between a strengthening heat transport and a strengthening ITF transport.

The spread of heat transport along the entry and exit passages of the Makassar Strait is shown in Figure 4c. Point A, The North Sulawesi Sea, as the initial gate of the ITF water mass, shows a value of -0.5 To +1.0 PW. Meanwhile, in the middle, along the Makassar Strait, to be precise, around the waters near Central Sulawesi, it shows a value of -1.5 PW. Heat transport in the Labani Channel area tends to show a value of -3.5 PW.

Heat transport along the Lifamatola Strait appears to be weaker than in the Makassar Strait. Heat transport increases and decreases along its propagation in Figure 4c. When heat transport passes through Halmahera Waters, it appears to have values ranging from -0.2 PW to -0.8 PW. Heat transport in the

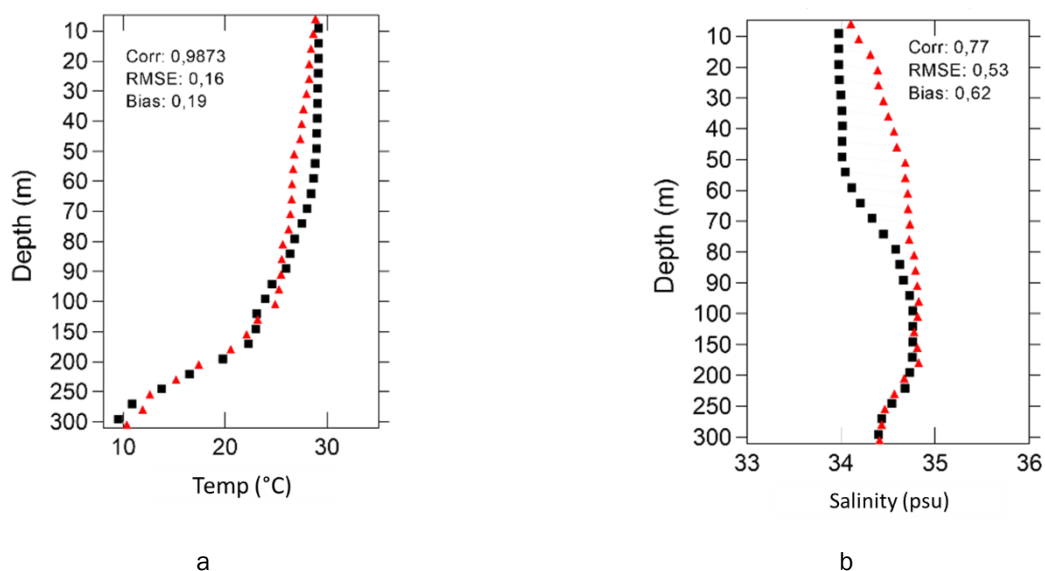


Figure 3. Validation by CMEMS vs PFL (a) Temperature (b) Salinity. Red triangle is reanalysis data and black square is observation data

Table 2. Lag correlation of heat transport vs ENSO

Location	Lag correlation	
	La Niña	El Niño
Makassar Strait	3-4 months	7-8 months
Lifamatola Strait	3-4 months	7-8 months

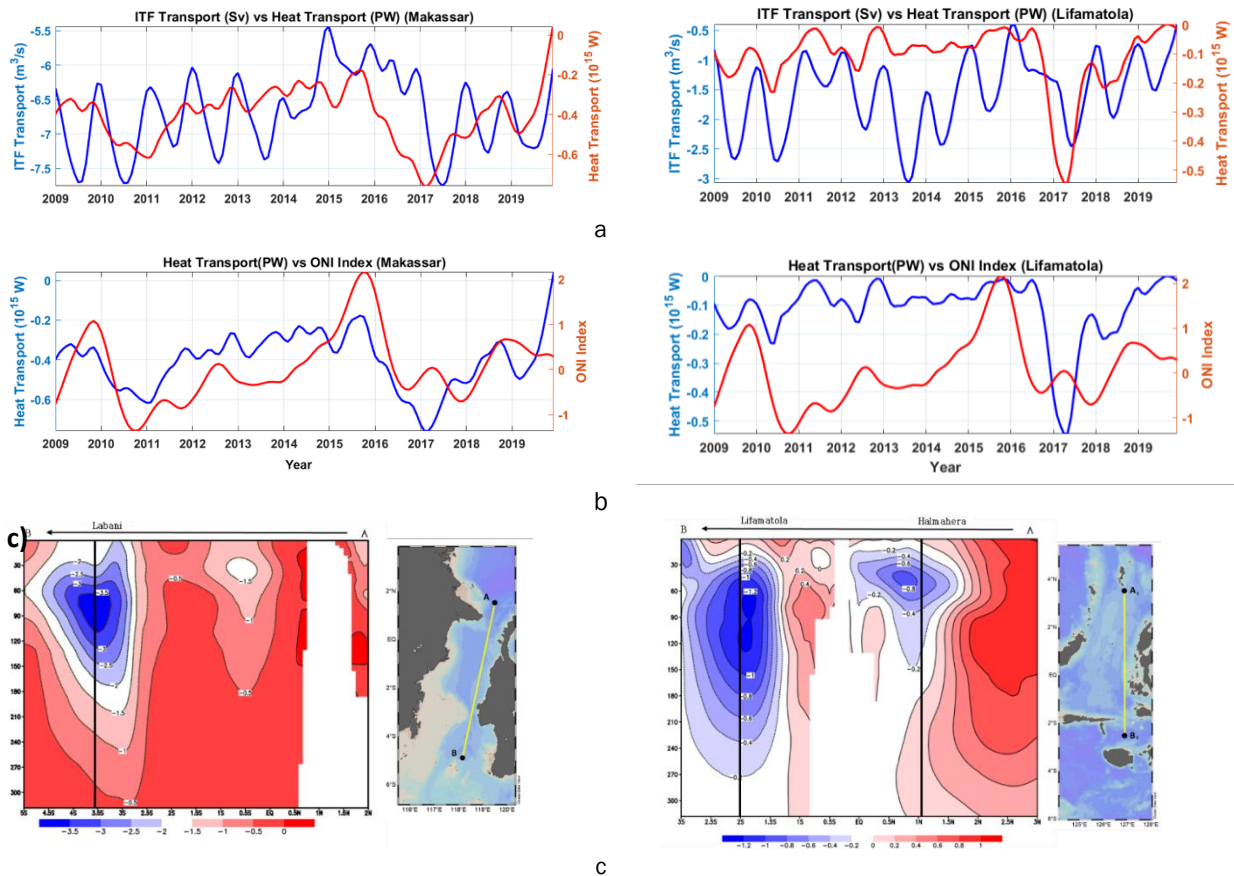


Figure 4. ITF transport (Sv) and heat transport (PW = 10^{15} Watt) in the (a) Makassar Strait (b) Lifamatola Strait. Propagation of heat transport in (c, left) Makassar Strait (c, right) Lifamatola Strait. Two transports are done by low pass filter using a cut-off of 13 months.

Lifamatola Strait shows a value of -0.4 PW to -1.2 PW. The two analyses involving the two straits show that the heat transport flowing into the Banda Sea is strongly influenced by location and its variability, namely ENSO. Table 2 shows the lag correlation of ENSO variability with the ONI index and heat transport in the two straits. The results of the lag correlation show that heat transport in the Makassar Strait and Lifamatola Strait during La Niña tends to experience delays with a lag time of 3–4 months.

Meanwhile, heat transport during La Niña (El Niño) has a lag time of 3-4 (7–8) months (Table 2). This difference is caused by different locations in terms of distance, which determines the propagation of heat transport to the Banda Sea.

Relationship of ENSO and influences in the Banda Sea

The effect of heat transport from the Makassar Strait and Lifamatola Strait is seen based on ocean parameters such as sub-surface salinity and mixed layer depth. Power spectral density (PSD) is used to determine the loop period of a parameter based on an event ($\text{year} \cdot \text{cycle}^{-1}$). The repetition period of the occurrence of the salinity parameter is shown in Figure 7a. The results of the salinity parameter with an average depth of 0-300 m are affected by inter-annual variability. This pattern can be seen in the power PSD, with the x-axis timeframe showing a loop of 3 years.

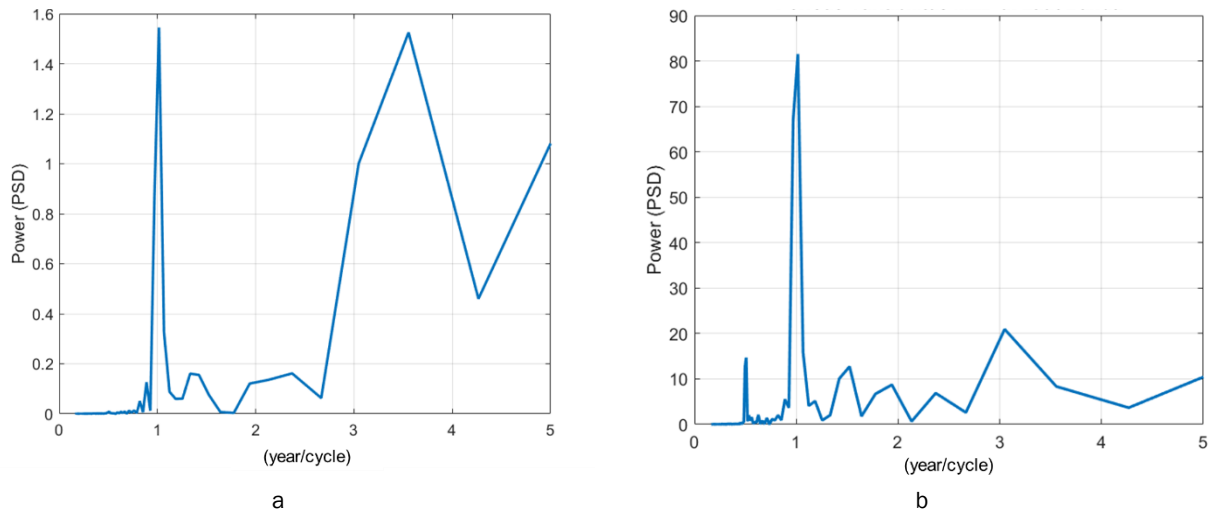


Figure 7. Probability Spectral Density (PSD) on (a) salinity and (b) MLD.

Change the salinity in the Banda Sea is one of the impacts caused by the water mass carried by ITF before heading to the Indian Ocean (Hu and Sprintall, 2016). Another variable found in the PSD results is seasonality. This is visible on the second high line after one year of repetition. The west and east monsoons that blow throughout the year cause disturbances in weather and ocean conditions (Zakir *et al.*, 2010).

Meanwhile, the mixed layer depth (MLD) parameter shown in Figure 7b shows that seasonal variability is more dominant. Furthermore, the northwest and southeast monsoons, which blow once every half year, cause faster fluctuations in the mixing layer due to temperature differences to a certain depth. Warm temperatures during the northwest monsoon cause the MLD to become thicker, and vice versa during the southeast monsoon (Sprintall *et al.*, 2012). Another variable affecting MLD in the Banda Sea is the ENSO phenomenon, which is identified through the interannual period (1 year). Physically, the ENSO causes upwelling in the eastern Indonesian waters so that the MLD becomes deep, whereas, during La Niña, it tends to experience downwelling in the Banda Sea (Atmadipoera *et al.*, 2018).

The heat transport flowing from the Pacific Ocean through the straits into Indonesian waters impacts changes in heat and salinity in the Banda Sea. Research conducted by Hu and Sprintall (2016) identified the role of salinity, which coincided with ITF transport, where it is known that the lag time is around 7-8 months until it heads to the Banda Sea. Salinity has a relationship with sea heat. Salinity, which tends to be high, is caused by cooling, high density, and a low precipitation rate, whereas low salinity is caused by heating, low density, and a high

precipitation rate (Firdaus, 2018; Herwindya *et al.*, 2018; Ratnawati *et al.*, 2018). Based on Figure 8a left, the first mode EOF value is 59.67% of the total variant. The area in the western part of the Banda Sea shows a lower traffic anomaly than in the middle of the Banda Sea. Figure 8b left shows a comparison of the value of the salinity anomaly in the Banda Sea with the ONI index. In 2010-2011, the La Niña phenomenon occurred, which caused the salinity conditions around the Banda Sea to decrease, along with the negative ONI index. Meanwhile, in 2015 and 2016, an El Niño phenomenon resulted in a positive salinity anomaly and a positive ONI index. Sprintall *et al.* (2009) conducted research that confirmed this condition. Then, in 2017-2018, the conditions for La Niña events were seen, one of which coincided with Tropical Cyclone Lili in 2019.

Meanwhile, mixed layer analysis (MLD) using the EOF method by first mode is 58.93% of the total variance (Figure 8a right). MLD plays a role in the stratification conditions of the oceans on the surface, controls the weather, and identifies surface water masses (Lin *et al.*, 2013). The ENSO phenomenon affects MLD in the Banda Sea (Hutabarat *et al.*, 2018). Figure 8b right shows a graph of the temporal fluctuation of the MLD anomaly in the Banda Sea. In 2010–2011, which was a La Niña event, positive MLD anomaly conditions were identified. In 2015–2016, an El Niño caused a negative MLD anomaly. Whereas in 2017-2018, there was a La Niña, which caused a positive MLD anomaly. Physically, an MLD that experiences a positive anomaly will thicken the layer, which is likely to delay the mixing and surface warming processes. Conversely, a negative MLD anomaly indicates a thinning of the depth layer, which causes surface conditions to have cooler

temperatures than during La Niña. The lag time analysis shows a positive correlation of 0.5 and a delay of 6–8 months. While the negative correlation is -0.3 and precedes it by 3–4 months. This means that when the El Niño phenomenon occurs, the MLD anomaly will decrease and have a relationship of about 6–8 months apart, while at La Niña, the MLD anomaly will increase with a gap of 3–4 months.

The sub-surface temperature profile in 2010–2011 experienced an increase marked in red with values around 30 °C, while in 2015–2016, cooler temperatures around 25 °C were seen (Figure 9a). This pattern indicates that the sub-surface temperature conditions in the Banda Sea during the La Niña tend to increase. As explained by the EOF method on the previous SST parameter, the sea surface temperature (SST) will experience an increase during the La Niña. It will affect the time delay, which ranges from 3 to 4 months. In addition, this proves that the sub-surface temperature during La Niña will cause the MLD to become thicker and that frequent mixing occurs so that the SST increases. Vranes *et al.* (2002) suggested that the heat carried by the water mass from the Pacific

Ocean affects the heat budget in the East Indian Ocean. Meanwhile, in the sub-surface salinity parameter shown in Figure 9b, there is a contour with a value of 35 PSU in the surface area during El Niño events. Whereas in the case of La Niña, it has a value of around 32 PSU (Figure 8b). Salinity values during El Niño events tend to increase compared to those during La Niña. During El Niño, the Banda Sea area is drier and experiences a deficit of precipitation and a cooler SST. This causes the surface layer's mixing (MLD) process to experience thinning. Conversely, during the La Niña, the Banda Sea area tends to experience increased temperatures, precipitation, and thickened MLD.

Ocean heat content in the Banda Sea

An increase in OHC was also found during the MAM period (Figure 10), which was $2,3 \times 10^{10}$ Joules. OHC during the MAM season is higher than in the DJF, JJA, and SON seasons. This increase in OHC is comparable to the results of EOF in MLD. The heat contained in the ocean can cause the surrounding air pressure to decrease so that convective clouds gather and can form tropical storm depressions (Lin

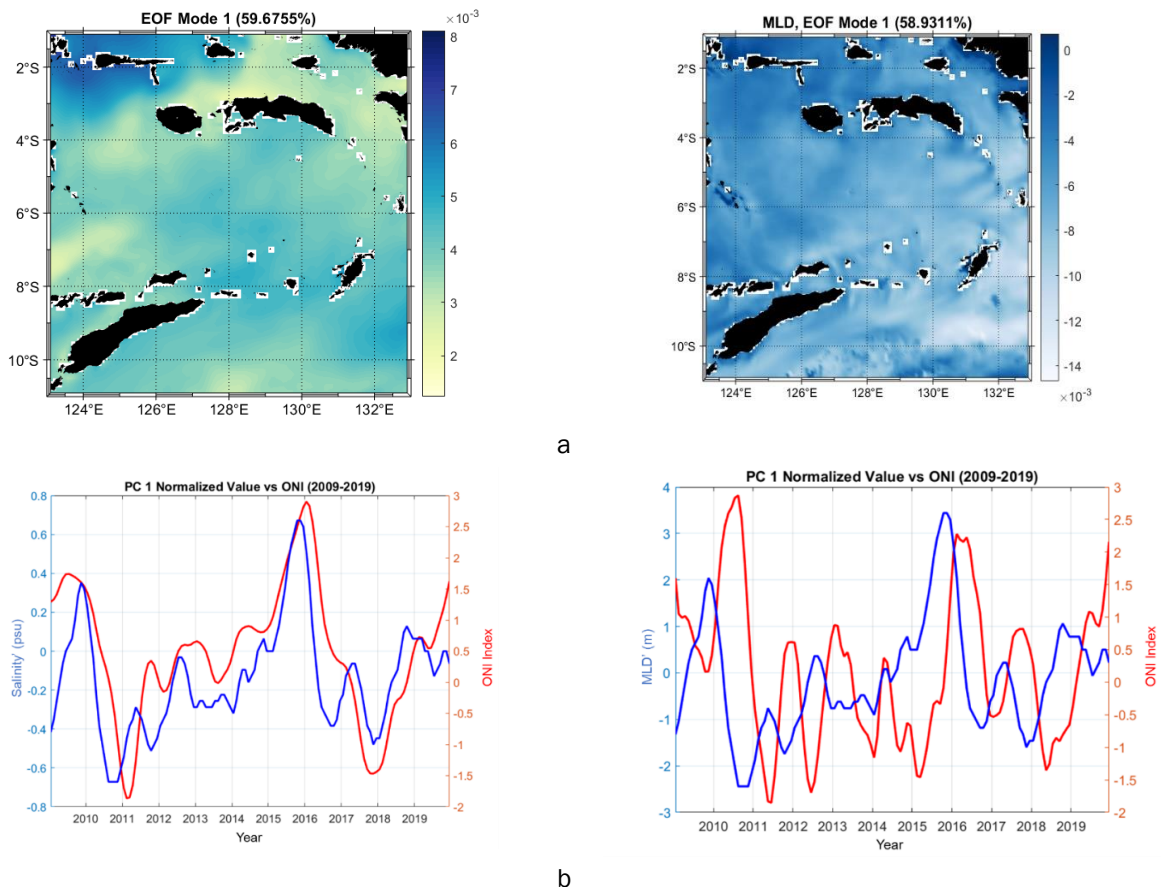


Figure 8. (a) The results of the first mode using the Empirical Orthogonal Function (EOF) method for salinity (left) and mixed layer depth (MLD) (right) (b) Comparison of the two parameters with the ONI index.

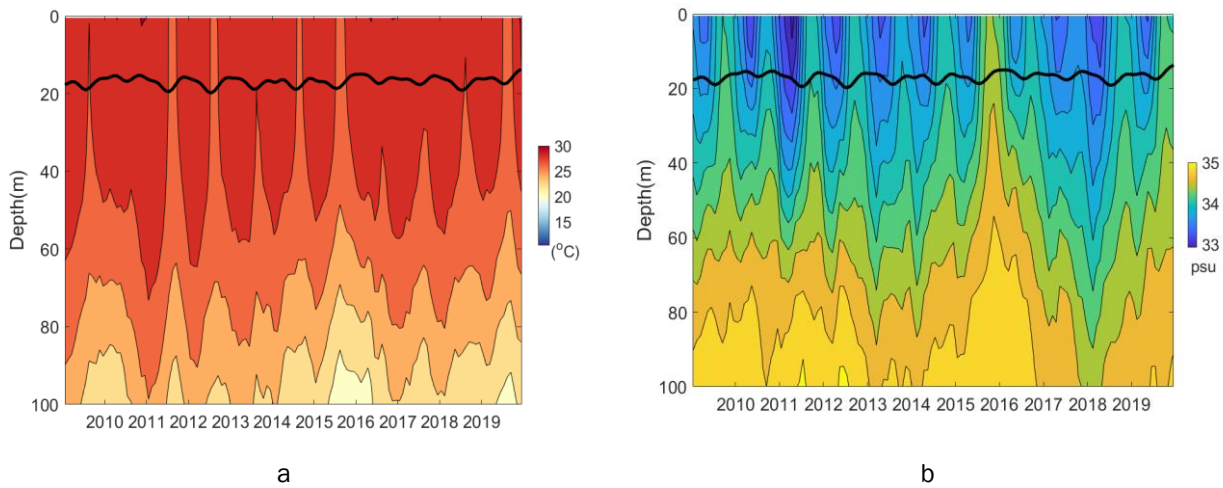


Figure 9. Cross section of (a) sub-surface temperature (b) salinity. Black line is depth of MLD.

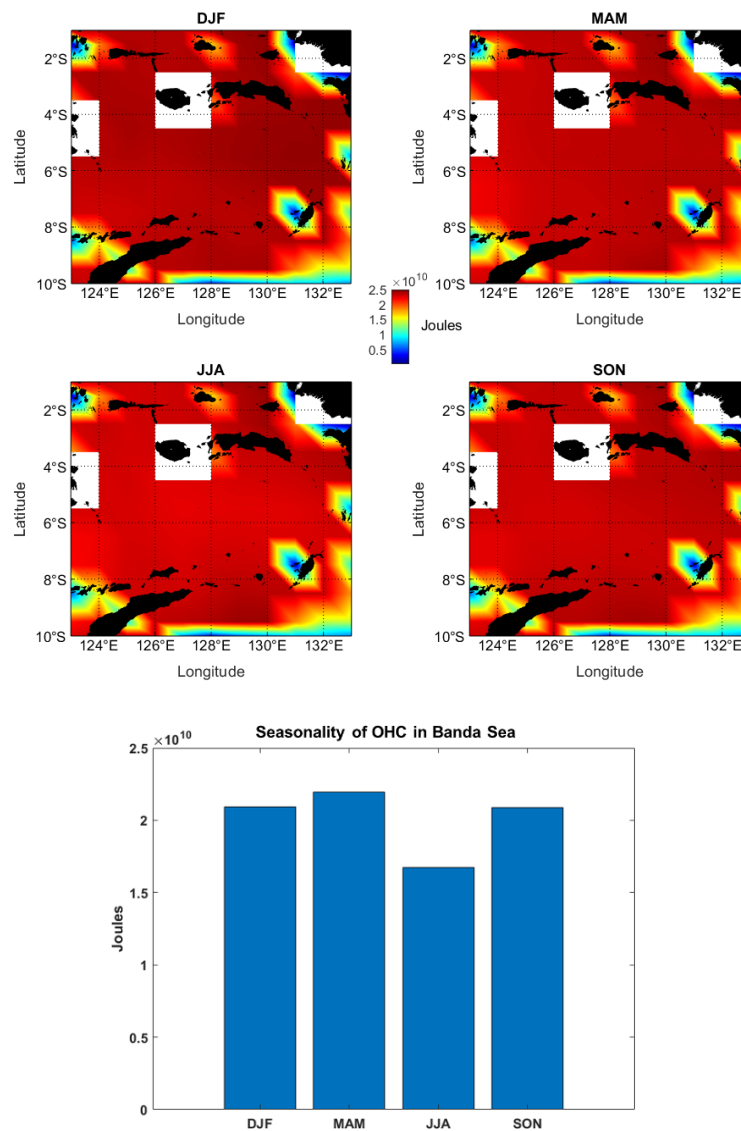


Figure 10. Seasonality of ocean heat content (OHC) in Banda Sea on December-January-February (DJF), March-April-May (MAM), June-July-August (JJA), September-October-November (SON)

et al., 2013). In addition, another effect from the Rossby wave is the accumulation of water column thrusters in the West Pacific region towards Indonesian waters. Sea surface height along 125°E to 140°W can indicate the propagation of Rossby waves. The El Niño generates wind bursts toward the westerlies (east) to form Kelvin waves that head to the coast of South America (McPhadden et al., 2020). Furthermore, the resulting bias is a wave propagating towards the west, called the Rossby wave. The Rossby wave acts as a collection of water column thrusters in the West Pacific region, propelling it towards Indonesian waters.

When the ENSO occurs, the water column in Indonesian waters experiences a decrease in elevation. This condition weakens the ITF transport and heat transport. On the other hand, during the La Niña, the water column tends to increase due to the strengthening of the Rossby waves towards the west, which causes ITF transport and heat transport to strengthen.

Conclusion

ITF transport in the Makassar Strait tends to have values between -4 Sv (during El Niño) and -7.5 Sv (during La Niña). Meanwhile, in the Lifamatola Strait, ITF's transport tends to experience of -0,5 Sv (during El Niño) and -3,5 Sv (during La Niña). This dynamic occurs because, during El Niño, the water column is higher in the Central Pacific Ocean. In contrast, during La Niña, the water column is higher in the West Pacific Ocean. The relationship between heat transport and ITF transport is very close. The same pattern between both shows this. Heat transport will strengthen during La Niña and weaken during El Niño. The EOF method results in the value of the first mode variant in MLD has an inverse relationship with the ENSO phenomenon. Meanwhile, the sub-surface salinity parameter has a relationship that is directly proportional to the ENSO phenomenon. As a result, the impact of heat transport propagation, comparable to ITF transport, is OHC fluctuations in the Banda Sea. The maximum OHC occurs during the MAM season, while the minimum OHC occurs during the JJA season.

Acknowledgments

This research is part of projects titled "Korea-Indonesia Marine Technology Cooperation Research Center (20220512)" and "Ocean and Coastal Basic Survey and Capacity Enhancement in Cirebon, Indonesia (PG53340)" which are funded by the Ministry of Oceans and Fisheries, Korea. Thanks to

Bandung Institute of Technology for their support and Evita Esmeralda for mathematics solution on this research.

References

- Atmadipoera, A.S., Khairunnisa, Z. & Kusuma, D.W. 2018. Upwelling characteristics during El Niño 2015 in Maluku Sea, *IOP Conf. Ser. Earth Environ. Sci.*, 176(1): p.012018. <https://doi.org/10.1088/1755-1315/176/1/012018>.
- Ffield, A. & Gordon, A.L. 1992. Vertical mixing in the Indonesian thermocline. *J. Physical Oceanogr.*, 22(2): 184–195. [https://doi.org/10.1175/1520-0485\(1992\)022<0184:VMITIT>2.0.CO;2](https://doi.org/10.1175/1520-0485(1992)022<0184:VMITIT>2.0.CO;2).
- Firdaus, M.L. 2018. Physical properties and nutrients distribution of seawater in the Banda Sea – Indonesia, *IOP Conf. Ser.:Earth Environ. Sci.*, 184(1): p.012011. <https://doi.org/10.1088/1755-1315/184/1/012011>.
- Gordon, A.L. & McClean, J.L. 1999. Thermocline stratification of the Indonesian Seas: Models and observations, *J. Physical Oceanogr.*, 29: 198–216. [https://doi.org/10.1175/1520-0485\(1999\)029<0198:TSOTIS>2.0.CO;2](https://doi.org/10.1175/1520-0485(1999)029<0198:TSOTIS>2.0.CO;2).
- Gordon, A. & Susanto, R. 2001. Banda Sea surface-layer divergence, *Ocean Dyn.*, 52: 2–10. <https://doi.org/10.1007/s10236-001-8172-6>.
- Gordon, A.L., Sprintall, J., Van Aken, H.M., Susanto, D., Wijffels, S., Molcard, R. & Wirasantosa, S. 2010. The Indonesian throughflow during 2004–2006 as observed by the INSTANT program, *Dynamics of Atmospheres and Oceans*, 50(2): 115–128. <https://doi.org/10.1016/j.dynatmoce.2009.12.002>.
- Gordon, A.L., Huber, B. A., Metzger, E.J., Susanto, R.D., Hurlburt, H.E. & Adi, T.R. 2012. South China Sea throughflow impact on the Indonesian throughflow, *Geophys. Res. Lett.*, 39: L11602. <https://doi.org/10.1029/2012GL052021>.
- Haryanto, Y., Florida, N., Purnama, D.R., Pradita, Nindya, I., Saveira, S., Suryo, A., Hananto, N., Li, S. & Susanto, R. 2021. Effect of Monsoon Phenomenon on Sea Surface Temperatures in Indonesian Throughflow Region and Southeast Indian Ocean, *Xinan Jiaotong Daxue Xuebao*, 56: 914-923. <https://doi.org/10.35741/issn.0258-2724.56.6.80>.
- Herwindya, A.Y., Sopardjo, A.H. & Aldrian, E. 2018. The effect of the Pacific Ocean water mass on

- water and climate around Maluku, *AIP Conf. Proc.*, 2023: p.020203. <https://doi.org/10.1063/1.5064200>.
- Hu, S. & Sprintall, J. 2017. Observed strengthening of interbasin exchange via the Indonesian seas due to rainfall intensification, *Geophys. Res. Lett.*, 44: 1448–1456. <https://doi.org/10.1029/2016GL072494>.
- Hu, S. & Sprintall, J. 2016. Interannual variability of the Indonesian Throughflow: The salinity effect, *J. Geophys. Res. Oceans*, 121: 2596–2615. <https://doi.org/10.1002/2015JC011495>.
- Hutabarat, M.F., Purba, N.P., Syamsuddin, M.L. & Kuswardani, A.R.T.D. 2018. Variabilitas Lapisan Termoklin terhadap Kenaikan Mixed Layer Depth (MLD) di Selat Makassar, *J. Perikanan dan Kelautan Unpad*, 9: p.1.
- Lin, I.I., Goni, G. J., Knaff, J.A., Forbes, C. & Ali, M.M. 2013. Ocean heat content for tropical cyclone intensity forecasting and its impact on storm surge, *Natural Hazards*, 66(3): 1481–1500. <https://doi.org/10.1007/s11069-012-0214-5>.
- Meyers, G. 1996. Variation of Indonesian throughflow and the El Niño-Southern Oscillation, *Geophys. Res. Lett.*, 101(C5): 12255–12263. <https://doi.org/10.1029/95JC03729>.
- Nanlohy, P., Nusaly, M., Eleewajaan, A. A., Luturmas, R.W., Latue, A.P., Supusepa, F., Lokollo, R., Andayani, H. & Elim, H. I. 2018. Variabilitas transport Volume Massa Air di Laut Banda Bagian Barat, *J. Multidisciplinary Application on Philosophy Sci.*, 1(1): 23-29. <https://doi.org/10.30598/JAMFASvol1iss1pp24-29y2018>.
- Napitu, A.M., Pujiana, K. & Gordon, A.L. 2018. The Madden-Julian Oscillation's impact on the Makassar Strait surface layer transport, *J. Geophys. Res.: Oceans*, 124: 3538–3550. <https://doi.org/10.1029/2018JC014729>.
- Nugroho, A.D. & Muzaki, N.H. 2022. Study of surface and vertical sea temperatures during the process of tropical cyclone formation in the territory of Indonesia (case study 2019-2021), *IOP Conf. Ser. Earth Environ. Sci.*, 989: 012006. <https://doi.org/10.1088/1755-1315/989/1/012006>.
- Pei, S., Shinoda, T., Steffen, J. & Seo, H. 2021. Substantial sea surface temperature cooling in the Banda Sea associated with the Madden-Julian Oscillation in the boreal winter of 2015. *J. Geophys. Res.: Oceans*, 126: p.e2021JC017226. <https://doi.org/10.1029/2021JC017226>
- Pujiana, K., Gordon, A.L., Metzger, E.J. & Field, A.L. 2012. The Makassar Strait pycnocline variability at 20–40 days, *Dynam. Atmos. Ocean.*, 53-54: 17–35. <https://doi.org/10.1016/j.dynatmoce.2012.01.001>.
- Purwanto, Sugianto, D.N., Zainuri, M., Permatasari, G., Atmodjo, W., Rochaddi, B., Ismanto, A., Wetchayont, P. & Wirasatriya, A. 2021. Seasonal Variability of Waves Within the Indonesian Seas and Its Relation With the Monsoon Wind, *Ilmu Kelautan: Indonesian Journal of Marine Sciences*, 26(3): 189-196. <https://doi.org/10.14710/ik.ijms.26.3.189-196>.
- Ratnawati, H.I., Aldrian, E. & Soepardjo, A.H. 2018. Variability of evaporation-precipitation (E-P) and sea surface salinity (SSS) over Indonesian maritime continent seas, *AIP Conf. Proc.*, 2023: p.020252. <https://doi.org/10.1063/1.5064249>
- Roman-Stork, H.L. Subrahmanyam, B. & Murty, V.S. N. 2020. The role of salinity in the southeastern Arabian Sea in determining monsoon onset and strength, *J. Geophys. Res.: Oceans*, 125(1): e2019JC015592. <https://doi.org/10.1029/2019JC015592>.
- Masoleh, V.C. & Atmadipoera, A.S. 2018. Coherence of transport variability along outer Banda Arcs, *IOP Conf. Ser. Earth Environ. Sci.*, 176(1): p.012012. <https://doi.org/10.1088/1755-1315/176/1/012012>.
- McPhaden, M.J., Lee, T., Fournier, S. & Balmaseda, M.A. 2020. ENSO Observations, El Niño Southern Oscillation in a Changing Climate. Geophysical Monograph Series. <https://doi.org/10.1002/9781119548164.ch3>
- Sotillo, M. G., Mourre, B., Mestres, M., Lorente, P., Aznar, R., García-León, M., Liste, M., Santana, A., Espino, M and Álvarez, E. 2021. Evaluation of the Operational CMEMS and Coastal Downstream Ocean Forecasting Services During the Storm Gloria (January 2020), *Front. Mar. Sci.*, 8: p.644525. <https://doi.org/10.3389/fmars.2021.644525>.
- Sprintall, J., Wijffels, S.E., Molcard, R. & Jaya, I. 2009. Direct estimation of the Indonesian throughflow entering the Indian Ocean: 2004–2009, *J. Geophys. Res.*, 114: 1–19. <https://doi.org/10.1029/2008JC005257>.
- Sprintall, J. & Revelard, A. 2014. The Indonesian Throughflow response to Indo-Pacific climate

- variability, *J. Geophys. Res.: Oceans*, 119: 1161-1175. <https://doi.org/10.1002/2013JC009533>.
- Sulaiman. 2008. Turbulensi Laut Banda (Studi Pendahuluan ARLINDO Microstructure), Lembaga Ilmu Pengetahuan Indonesia (LIPI).
- Vranes, K., Gordon, A.L. & Field, A. 2002. The heat transport of the Indonesian Throughflow and implications for the Indian Ocean heat budget, *Deep-Sea Res. II: Topical Stud. Oceanogr.*, 49(7-8): 1391-1410. [https://doi.org/10.1016/S0967-0645\(01\)00150-3](https://doi.org/10.1016/S0967-0645(01)00150-3)
- Wang, B. & Zhou, X. 2008. Climate variation and prediction of rapid intensification in tropical cyclones in the western North Pacific, *Meteorology and Atmospheric Physics*, 99(1-2): 1-16. <https://doi.org/10.1007/s00703-006-0238-z>.
- Wijaya, A. Priyono, B. & Mahdalena, N. C. 2018. Karakteristik Spasial Temporal Kondisi Oseanografi Laut Banda dan Hubungannya dengan Potensi Sumberdaya Perikanan, *J. Fisheries Mar. Res.*, 2(2): 75-85. <https://doi.org/10.21776/ub.jfmr.2018.002.02.4>